Table 2
Neurologic symptoms.

Patient	Initial neurological symptom	LOC at onset	Sz at onset of AE	Sz after admission	Delirious behavior	Interval from initial symptom to coma (h)
1	Mildly altered MS	Mildly altered MS	2 brief Szs	None	Shouting in a loud voice and t acting violently	6
2	Delirious behavior	Mildly altered MS	None	2 brief seizures	Meaningless speech,	3
3	Brief seizure	None	1 brief Sz	None	None	3
4	Tremulous movement	None	None	None	None	2
5	Delirious behavior	Mildly altered MS	None	None	Meaningless speech	6
6	Brief seizure	Mildly altered MS	1 brief Sz	2 brief seizures	None	3
7	Delirious behavior	Mildly altered MS	None	None	Meaningless speech	1
8	Semicoma	Semicoma	None	Frequent subclinical Szs	None	2
9	Status epilepticus	Coma	Status epilepticus	Status epilepticus	None	1
10	Delirious behavior	Mildly altered MS	Status epilepticus	None	Meaningless speech	4
11	Brief seizure	Mildly altered MS	1 brief Sz	Status epilepticus	None	1
12	Brief seizure	Mildly altered MS	1 brief Sz	1 brief Sz	None	1
13	Brief seizure	None	1 brief Sz	None	None	9
14	Delirious behavior	None	None	1 brief Sz	Meaningless speech, acting violently	11
15	Delirious behavior	Mildly altered MS	1 brief Sz	None	Meaningless speech, acting disorientedly	5
16	Brief seizure	Coma	1 brief Sz	None	None	1
17	Coma	Coma	None	None	None	0
18	Status epilepticus	Coma	Status epilepticus	Status epilepticus	None	1
19	Coma	Coma	None	None	None	0
20	Status epilepticus	Coma	Status epilepticus	Status epilepticus	None	1

LOC, loss of consciousness; Sz, seizure; AE, acute encephalopathy; MS, mental status.

Table 3
Brain CT.

Patient	Initial CT				Subsequent CT			
	Hours after admission	Findings			Hours after admission	Findings		
		Brain edema	G–W differentiation	Low densities		Brain edema	G–W differentiation	Low densities
1	3	Mild	Preserved	None				
2	0	Mild	Mildly blurred	Brainstem	4	Marked	Blurred	Brainstem, thalamus
3	20	Marked	Blurred	Brainstem, basal ganglia, thalamus				
4	12	Marked	Blurred	Brainstem, thalamus				
5	1	Mild	Preserved	Brainstem				
6	AI	Marked	Blurred	None				
7	1	Mild	Preserved	Brainstem				
8	1	Marked	Blurred	Brainstem, basal ganglia, thalamus				
9	1	None	None	None	36	Marked	Blurred	None
10	2	Mild	Preserved	Brainstem	240	Marked	Blurred	Brainstem
11	1	Mild	Preserved	None	9	Marked	Blurred	None
12	12	Marked	Blurred	None				
13	12	Marked	Blurred	Brainstem, basal ganglia	44	Marked	Blurred	Brainstem, basal ganglia
14	2	None	None	None				
15	1	Mild	Mildly blurred	Brainstem	5	Marked	Blurred	Brainstem, thalamus
16	Not done							
17	1	Marked	Blurred	Brainstem				
18	1	None	None	None	120	Marked	Blurred	Brainstem
19	2	None	None	None	48	Marked	Blurred	None
20	1	None	None	None	96	Marked	Blurred	Brainstem, basal ganglia

AI, autopsy imaging; G–W, gray–white matter.

of acute encephalopathy. All of them required intensive life support including artificial ventilation and tube feeding.

5. Discussion

Our report describes the largest case series of the severe form of acute encephalopathy associated with pH1N1. The information in our study will be useful for understanding the features of the severe form of acute encephalopathy associated with seasonal influenza, although there are some differences in pediatric deaths between IAE due to A/H1N1 pdm 2009 and that due to the seasonal influenza virus. Although there have been several case series and patient reports on neurological complications of pH1N1 from many countries, including acute encephalopathy,[12–29] reports on children who died or who survived with very severe sequelae are limited.[12–17]

A fulminant clinical course with rapidly progressing coma is a remarkable feature in our patients. In most patients, coma developed within 6 h of onset, although the neurological manifestations at onset were relatively mild, including a brief seizure or delirious behavior. Such mild neurological symptoms are often observed in children without acute encephalopathy.[31,32] Therefore, the early recognition of acute encephalopathy is difficult, and rapid worsening of neurological symptoms cannot always be expected. At present, early intervention for the patients with such fulminant encephalopathy is difficult because of its devastating nature. Therefore, future studies should be directed to the prevention of acute encephalopathy, including vaccination.

Note that a large majority of our patients had no pre-existing conditions. Several reports on acute encephalopathy or neurological complications of pH1N1 found that the majority of children with acute encephalopathy had pre-existing conditions. According to Ekstrand, most patients with neurological complications had an underlying medical condition (83%), primarily neurological conditions (66%).[12] Pre-existing conditions were present in about a half of the patients in some reports,[13,16,18] whereas no pre-existing conditions were seen in several case reports and case series of acute encephalopathy with pH1N1.[14,15,17,19–24] These conflicting data indicate that further studies are necessary to clarify the relationship between pre-existing conditions and acute encephalopathy.

Frequent brainstem involvement was an important feature in our patients. Brainstem lesions on CT were seen in 12 of the 20 patients in our cohort. Brainstem lesions were also described in at least seven patients in previous reports on acute encephalopathy or neurological complications of pH1N1,[14–18,23,25] and three of these patients died.[14,15,17] We believe that the brainstem involvement contributed to the dismal outcomes. Our previous study showed that the presence of brainstem lesions was correlated with a poor outcome in children with acute necrotizing encephalopathy (ANE).[33] The outcome is also poor for children with brainstem encephalitis caused by enterovirus 71.[34]

Five of our patients had thalamic lesions in addition to brainstem lesion. These neuroimaging findings are compatible to ANE as proposed by Mizuguchi.[35] The hallmark of ANE is multifocal, symmetric brain lesions affecting the bilateral thalami, brainstem, cerebral white matter, and cerebellar medulla. The majority of described ANE patients were of Asian origin. However, there have been increasing reports of ANE with pH1N1 from North America and Europe.[13,14,16,18,20,22,23,25] This suggests that pH1N1 has a predilection to ANE. At present, hypercytokinemia and hyperpermeability of both the blood–brain barrier and the capillary walls of the brain are considered to be closely related to the pathogenesis of ANE.[36–38] Some authors suggested increased cytokine production due to A/H1N1 pdm 2009 infection,[39] whereas others reported the opposite.[40] Further studies are necessary to clarify the relationship between 2009 pandemic flu and a possible increase in pediatric ANE.

It is interesting that delirious behavior was the initial neurological symptom in several patients. Nagao et al. investigated clinical variables in children with IAE and observed delirious behavior in 36 of 430 (8.3%) patients.[41] Of the 93 patients who died in that study, only four (4.3%) had shown delirious behavior.[41] Our previous study found that eight of 38 children with ANE showed delirious behavior as an early neurological manifestation.[42] All but one patient with delirious behavior as the initial neurological symptom had brainstem lesions. These data suggest that an onset with delirious behavior is related to brainstem involvement.

Protection by vaccination is a very important issue. However, no study has examined the protective effect of vaccination against IAE. This is due to the lack of reliable data on vaccinated children who had influenza but did not have severe complications such as acute encephalopathy and severe pneumonia. Prospective studies are necessary to solve this important problem.

There are some limitations to this study. First, there are no national data on severe complications associated with seasonal influenza. Therefore, a comparison of pH1N1 and seasonal influenza is difficult. The chief author compared historical data for patients with seasonal flu and patients with pH1N1 using data compiled by a local group of pediatric neurologists.[43] That study showed that acute encephalopathy with pH1N1 occurred mainly among children 6 years of age or older, and the outcome was worse in this age group compared with acute encephalopathy with seasonal influenza. However, it is unclear whether these results can be applied to a larger cohort. The lack of information from autopsied cases is another limitation. In Japan, it is quite difficult to obtain the pathological findings from autopsied cases because of medicolegal or ethical issues. The lack of a detailed evaluation of metabolic conditions is also a shortcoming of our study. It is not always easy to distinguish between acute encephalopathy and decompensation due to metabolic diseases triggered by infection.

In conclusion, the clinical course of the patients was characterized by an onset with mild neurological symptoms such as delirious behavior or a brief seizure, followed by rapid deterioration of consciousness into coma and then severe multi-organ failure. Head CT revealed marked cerebral edema often associated with brainstem or deep gray matter lesions.

Funding

This study is supported by the grants from the Ministry of Health, Labor, and Welfare of Japan (H21-Tokubetsu-027 and H22-Nanji-Ippan-049).

Competing interests

We have no conflict of interest in relation to this manuscript. We do not have any financial relationships with pharmaceutical companies, medical equipment manufacturers, biomedical device manufacturers, or any companies with significant involvement in the field of health care.

Ethical approval

This study is considered to be a public health activity and an approval from an ethics committee and informed consent were considered not to be required.

Acknowledgments

We thank all doctors who participated in the interview and surveillance for their contributions.

References

1. Morishima T, Togashi T, Yokota S, Okuno Y, Miyazaki C, Tashiro M, et al. Encephalitis and encephalopathy associated with an influenza epidemic in Japan. *Clin Infect Dis* 2002;**35**:512–7.
2. Nguyen-Van-Tam JS, Openshaw PJ, Hashim A, Gadd EM, Lim WS, Semple MG, et al. Risk factors for hospitalisation and poor outcome with pandemic A/H1N1 influenza: United Kingdom first wave (May–September 2009). *Thorax* 2010;**65**:645–51.
3. Webb SA, Pettilä V, Seppelt I, Bellomo R, Bailey M, Cooper DJ, et al. Critical care services and 2009 H1N1 influenza in Australia and New Zealand. *N Engl J Med* 2009;**361**:1925–34.
4. Kumar A, Zarychanski R, Pinto R, Cook DJ, Marshall J, Lacroix J, et al. Critically ill patients with 2009 influenza A (H1N1) infection in Canada. *JAMA* 2009;**302**:1872–9.
5. Echevarría-Zuno S, Mejía-Aranguré JM, Mar-Obeso AJ, Grajales-Muñiz C, Robles-Pérez E, González-León M, et al. Infection and death from influenza A H1N1 virus in Mexico: a retrospective analysis. *Lancet* 2009;**374**:2072–9.
6. Louie JK, Acosta M, Winter K, Jean C, Gavali S, Schechter R, et al. Factors associated with death or hospitalization due to pandemic 2009 influenza A (H1N1) infection in California. *JAMA* 2009;**302**:1896–902.
7. Libster R, Bugna J, Coviello S, Hijano DR, Dunaiewsky M, Reynoso N, et al. Pediatric hospitalizations associated with 2009 pandemic influenza A (H1N1) in Argentina. *N Engl J Med* 2010;**362**:45–55.
8. Lister P, Reynolds F, Parslow R, Chan A, Cooper M, Plunkett A, et al. Swine-origin influenza virus H1N1, seasonal influenza virus, and critical illness in children. *Lancet* 2009;**374**:605–7.
9. Yung M, Slater A, Festa M, Williams G, Erickson S, Pettila V, et al. Pandemic H1N1 in children requiring intensive care in Australia and New Zealand during winter 2009. *Pediatrics* 2011;**127**:e156–63.
10. Louie JK, Gavali S, Acosta M, Samuel MC, Winter K, Jean C, et al. Children hospitalized with 2009 novel influenza A (H1N1) in California. *Arch Pediatr Adolesc Med* 2010;**164**:1023–31.
11. Sachedina N, Donaldson LJ. Paediatric mortality related to pandemic influenza A H1N1 infection in England: an observational population-based study. *Lancet* 2010;**376**:1846–52.
12. Ekstrand JJ, Herbener A, Rawlings J, Turney B, Ampofo K, Korgenski EK, et al. Heightened neurologic complications in children with pandemic H1N1 influenza. *Ann Neurol* 2010;**68**:762–6.
13. Yıldızdaş D, Kendirli T, Arslanköylü AE, Horoz OO, Incecik F, Ince E, et al. Neurological complications of pandemic influenza (H1N1) in children. *Eur J Pediatr* 2011;**170**:779–88.
14. Lyon JB, Remigio C, Milligan T, Deline C. Acute necrotizing encephalopathy in a child with H1N1 influenza infection. *Pediatr Radiol* 2010;**40**:200–5.
15. Martin A, Reade EP. Acute necrotizing encephalopathy progressing to brain death in a pediatric patient with novel influenza A (H1N1) infection. *Clin Infect Dis* 2010;**50**:e50–2.
16. Kedia S, Stroud B, Parsons J, Schreiner T, Curtis DJ, Bagdure D, et al. Pediatric neurological complications of 2009 pandemic influenza A (H1N1). *Arch Neurol* 2011;**68**:455–62.
17. Lung DC, Lui WY, Ng HL, Lam DS, Que TL. Hemorrhagic shock and encephalopathy syndrome in a child with pandemic H1N1 2009 influenza virus. *Pediatr Infect Dis J* 2011;**30**:998–9.
18. Surana P, Tang S, McDougall M, Tong CY, Menson E, Lim M. Neurological complications of pandemic influenza A H1N1 2009 infection: European case series and review. *Eur J Pediatr* 2011;**170**:1007–15.
19. Rellosa N, Bloch KC, Shane AL, Debiasi RL. Neurologic manifestations of pediatric novel H1N1 influenza infection. *Pediatr Infect Dis J* 2011;**30**:165–7.
20. Baltagi SA, Shoykhet M, Felmet K, Kochanek PM, Bell MJ. Neurological sequelae of 2009 influenza A (H1N1) in children: a case series observed during a pandemic. *Pediatr Crit Care Med* 2010;**11**:179–84.
21. Webster RI, Hazelton B, Suleiman J, Macartney K, Kesson A, Dale RC. Severe encephalopathy with swine origin influenza A H1N1 infection in childhood: case reports. *Neurology* 2010;**74**:1077–8.
22. Bartynski WS, Upadhyaya AR, Petropoulou KA, Boardman JF, Influenza A. encephalopathy, cerebral vasculopathy, and posterior reversible encephalopathy syndrome: combined occurrence in a 3-year-old child. *Am J Neuroradiol* 2010;**31**:1443–6.
23. Mariotti P, Iorio R, Frisullo G, Plantone D, Colantonio R, Tartaglione T, et al. Acute necrotizing encephalopathy during novel influenza A (H1N1) virus infection. *Ann Neurol* 2010;**68**:111–4.
24. Iwata A, Matsubara K, Nigami H, Kamimura K, Fukaya T. Reversible splenial lesion associated with novel influenza A (H1N1) viral infection. *Pediatr Neurol* 2010;**42**:447–50.
25. Ormitti F, Ventura E, Summa A, Picetti E, Crisi G. Acute necrotizing encephalopathy in a child during the 2009 influenza A (H1N1) pandemia: MR imaging in diagnosis and follow-up. *Am J Neuroradiol* 2010;**31**:396–400.
26. Centers for Disease Control and Prevention (CDC). Neurologic complications associated with novel influenza A (H1N1) virus infection in children – Dallas, Texas, May 2009. *MMWR Morb Mortal Wkly Rep* 2009;**58**:773–8.
27. Gonzalez BE, Brust DG. Novel influenza A (H1N1) presenting as an acute febrile encephalopathy in a mother and daughter. *Clin Infect Dis* 2009;**49**:1966–7.
28. Ozkan M, Tuygun N, Erkek N, Aksoy A, Yıldız YT. Neurologic manifestations of novel influenza A (H1N1) virus infection in childhood. *Pediatr Neurol* 2011;**45**:72–6.
29. Thampi N, Bitnun A, Banner D, Rowe T, Kelvin DJ, Richardson SE, et al. Influenza-associated encephalopathy with elevated antibody titers to pandemic (H1N1) 2009 influenza. *J Child Neurol* 2011;**26**:501–6.
30. Okumura A, Nakagawa S, Kawashima H, Muguruma T, Saito O, Fujimoto J, et al. Causes of Pediatric Deaths Associated with the 2009 Pandemic Influenza A (H1N1) Virus infection in Japan. *Emerg Infect Dis* 2011;**17**:1993–2000.
31. Okumura A, Hayakawa F, Kato T, Suzuki M, Tsuji T, Fukumoto Y, et al. Callosal lesions and delirious behavior during febrile illness. *Brain Dev* 2009;**31**:158–62.
32. Fukumoto Y, Okumura A, Hayakawa F, Suzuki M, Kato T, Watanabe K, et al. Serum levels of cytokines and EEG findings in children with influenza associated with mild neurological complications. *Brain Dev* 2007;**29**:425–30.
33. Okumura A, Mizuguchi M, Kidokoro H, Tanaka M, Abe S, Hosoya M, et al. Outcome of acute necrotizing encephalopathy in relation to treatment with corticosteroids and gammaglobulin. *Brain Dev* 2009;**31**:221–7.
34. Lee TC, Guo HR, Su HJ, Yang YC, Chang HL, Chen KT. Diseases caused by enterovirus 71 infection. *Pediatr Infect Dis J* 2009;**28**:904–10.
35. Mizuguchi M. Acute necrotizing encephalopathy of childhood: a novel form of acute encephalopathy prevalent in Japan and Taiwan. *Brain Dev* 1997;**19**: 81–92.
36. Mizuguchi M, Yamanouchi H, Ichiyama T, Shiomi M. Acute encephalopathy associated with influenza and other viral infections. *Acta Neurol Scand* 2007;**115**(Suppl.):45–56.
37. Ichiyama T, Isumi H, Ozawa H, Matsubara T, Morishima T, Furukawa S. Cerebrospinal fluid and serum levels of cytokines and soluble tumor necrosis factor receptor in influenza virus-associated encephalopathy. *Scand J Infect Dis* 2003;**35**:59–61.
38. Aiba H, Mochizuki M, Kimura M, Hojo H. Predictive value of serum interleukin-6 level in influenza virus-associated encephalopathy. *Neurology* 2001;**57**:295–9.
39. Bermejo-Martin JF, Ortiz de Lejarazu R, Pumarola T, Rello J, Almansa R, Ramírez P, et al. Th1 and Th17 hypercytokinemia as early host response signature in severe pandemic influenza. *Crit Care* 2009;**13**:R201.
40. Osterlund P, Pirhonen J, Ikonen N, Rönkkö E, Strengell M, Mäkelä SM, et al. Pandemic H1N1 2009 influenza A virus induces weak cytokine responses in human macrophages and dendritic cells and is highly sensitive to the antiviral actions of interferons. *J Virol* 2010;**84**:1414–22.
41. Nagao T, Morishima T, Kimura H, Yokota S, Yamashita N, Ichiyama T, et al. Prognostic factors in influenza-associated encephalopathy. *Pediatr Infect Dis J* 2008;**27**:384–9.
42. Okumura A, Mizuguchi M, Aiba H, Tanabe T, Tsuji T, Ohno A. Delirious behavior in children with acute necrotizing encephalopathy. *Brain Dev* 2009;**31**:594–9.
43. Okumura A, Tsuji T, Kubota T, Ando N, Kobayashi S, Kato T, et al. Acute encephalopathy with 2009 pandemic flu: comparison with seasonal flu. *Brain Dev* 2012;**34**:13–9.

DOI:10.1111/irv.12032
www.influenzajournal.com

Letter to the Editor

Unexpected cardiopulmonary arrest associated with influenza: our experience during the 2009 pandemic in Japan

Akihisa Okumura,[a] Satoshi Nakagawa,[b] Hisashi Kawashima,[c] Takashi Muguruma,[b] Osamu Saito,[b] Jun-ichi Fujimoto,[b] Chiaki Toida,[b] Shuji Kuga,[b] Toshihiro Imamura,[b] Toshiaki Shimizu,[a] Naomi Kondo,[d] Tsuneo Morishima[e]

[a]Department of Pediatrics, Juntendo University Faculty of Medicine, Tokyo, Japan. [b]Division of Critical Care Medicine, National Center for Child Health and Development, Tokyo, Japan. [c]Department of Pediatrics, Tokyo Medical University School of Medicine, Tokyo, Japan. [d]Department of Pediatrics, Gifu University Graduate School of Medicine, Gifu, Japan. [e]Department of Pediatrics, Okayama University Graduate School of Medicine, Dentistry and Pharmaceutical Sciences, Okayama, Japan.
Correspondence: Akihisa Okumura, Department of Pediatrics, Juntendo University Faculty of Medicine, 2-1-1 Hongo, Bunkyo-ku, Tokyo 113-8421, Japan. E-mail: okumura@juntendo.ac.jp

Accepted 14 September 2012. Published Online 5 November 2012.
Keywords Pediatric death, preexisting conditions, unexpected cardiopulmonary arrest, 2009 pandemic influenza A (H1N1).

To the editor:
Our national survey of pediatric deaths associated with 2009 pandemic influenza A (H1N1) (pH1N1) infection revealed that unexpected cardiopulmonary arrest (CPA) was one of the leading cause of pediatric deaths in Japan.[1] Unexpected CPA associated with influenza can be underestimated due to difficulty in obtaining detailed information. We investigated the actual situation of unexpected CPA in association with pH1N1.

As of the end of March, 2010, 41 deaths associated with pH1N1 were identified among patients younger than 20 years old in Japan.[1] Unexpected CPA was defined as CPA without clear findings of respiratory failure, cardiomyopathy, or encephalopathy. We also excluded children with radiological findings consistent with encephalopathy and respiratory failure. Fifteen pediatric deaths were categorized as unexpected CPA.

There were nine boys and six girls. Median age was 43 months (range, 7–164 months). One patient had severe delay in psychomotor development. CPA occurred within the first 2 days after influenza onset in 12 patients. The site of CPA was home in 13 patients. One patient collapsed at a local outpatient clinic and the other had CPA during hospitalization. CPA was noticed in the daytime (7:00–18:00) in 11 patients. The interval between being witnessed alive and CPA was <30 minutes in seven patients. In four patients, CPA was noticed immediately after its occurrence. Emergency services transferred most patients to a hospital within 30 minutes after being called. Blood gas data on presentation were measured in 10 patients, and pH <7·0 was seen in nine patients and base excess <−20 mm in eight patients. Chest radiographs were obtained in 12 patients and showed mild infiltration in four and pulmonary edema in 1. Chest CT was performed in four patients but showed only mild and non-specific findings. Head CT was performed in eight patients; all were unremarkable.

Our study showed that unexpected CPA occurred mostly in previously healthy children without antecedent signs. This contrasts with pediatric deaths due to respiratory failure associated with pH1N1.[2–5] Thus, it is difficult to predict the occurrence of CPA. It is noteworthy that a majority of unexpected CPAs occurred during the daytime and the occurrence was noticed within a short interval. These results imply that CPA occurred within a few minutes and that their deaths cannot be attributable to a delay in the recognition. The cause of unexpected CPA in our patients is difficult to determine. Possible explanations may be latent myocardial involvement causing fatal arrhythmia or circulatory collapse,[6–8] and immune-mediated injury induced by hypercytokinemia.[9] An accumulation of postmortem pathological findings is important to elucidate the cause of unexpected CPA in patients with influenza.

Acknowledgements

We thank all doctors who participated in the interview and surveillance for their contributions. This study is supported by the grants from the Ministry of Health, Labour, and Welfare of Japan (H21-Tokubetsu-027, H22-Nanji-Ippan-049, and H24-Shinkou-Ippan-002). We do not have any financial relationships with pharmaceutical companies, medical equipment manufacturers, biomedical device manufacturers, or any companies with significant involvement in the field of health care.

Authors' contribution

AO wrote the first draft of the manuscript. AO, SN, and HK were the chief members of collaborative study group and conducted the study, interpreted the data, and made consensus regarding the cause of death. TM, OS, JF, CT, SK, and TI were the members of the collaborative study group. They visited the hospital and interviewed the attending pediatricians of the patient in cooperation with the chief members. ST, NK and TM supervised the study and corrected the manuscript.

Conflict of interest

All authors have no conflict of interest in relation to this manuscript.

References

1 Okumura A, Nakagawa S, Kawashima H *et al.* Deaths associated with pandemic (H1N1) 2009 among children, Japan, 2009–2010. Emerg Infect Dis 2011; 17:1993–2000.

2 Cox CM, Blanton L, Dhara R, Brammer L, Finelli L. 2009 Pandemic influenza A (H1N1) deaths among children – United States, 2009–2010. Clin Infect Dis 2011; 52(Suppl):S69–S74.

3 Sachedina N, Donaldson LJ. Paediatric mortality related to pandemic influenza A H1N1 infection in England: an observational population-based study. Lancet 2010; 376:1846–1852.

4 Yung M, Slater A, Festa M *et al.* Pandemic H1N1 in children requiring intensive care in Australia and New Zealand during winter 2009. Pediatrics 2011; 127:e156–e163.

5 Louie JK, Gavali S, Acosta M *et al.* Children hospitalized with 2009 novel influenza A (H1N1) in California. Arch Pediatr Adolesc Med 2010; 164:1023–1031.

6 Frank H, Wittekind C, Liebert UG *et al.* Lethal influenza B myocarditis in a child and review of the literature for pediatric age groups. Infection 2010; 38:231–235.

7 Tabbutt S, Leonard M, Godinez RI *et al.* Severe influenza B myocarditis and myositis. Pediatr Crit Care Med 2004; 5:403–406.

8 Gdynia G, Schnitzler P, Brunner E *et al.* Sudden death of an immunocompetent young adult caused by novel (swine origin) influenza A/H1N1-associated myocarditis. Virchows Arch 2011; 458: 371–376.

9 Landi KK, Coleman AT. Sudden death in toddlers caused by influenza B infection: a report of two cases and a review of the literature. J Forensic Sci 2008; 53:213–215.

MAJOR ARTICLE

Differences in Cytokine Production in Human Macrophages and in Virulence in Mice Are Attributable to the Acidic Polymerase Protein of Highly Pathogenic Influenza A Virus Subtype H5N1

Saori Sakabe,[1,5] Ryo Takano,[1] Tokiko Nagamura-Inoue,[2] Naohide Yamashita,[3] Chairul A. Nidom,[6] Mai thi Quynh Le,[7] Kiyoko Iwatsuki-Horimoto,[1] and Yoshihiro Kawaoka[1,4,5,8]

[1]Division of Virology, Department of Microbiology and Immunology, [2]Department of Cell Processing and Transfusion, Research Hospital, [3]Department of Advanced Medical Science, and [4]International Research Center for Infectious Diseases, Institute of Medical Science, University of Tokyo, and [5]ERATO Infection-Induced Host Responses Project, Saitama, Japan; [6]Faculty of Veterinary Medicine, Tropical Disease Centre, Airlangga University, Surabaya, Indonesia; [7]National Institute of Hygiene and Epidemiology, Hanoi, Vietnam; and [8]Department of Pathobiological Sciences, School of Veterinary Medicine, University of Wisconsin-Madison

(See the editorial commentary by Donis and Cox, on pages 208–10 and editorial commentary Hirsch, on page 207.)

Background. The pathogenesis of influenza A virus subtype H5N1 (hereafter, "H5N1") infection in humans is not completely understood, although hypercytokinemia is thought to play a role. We previously reported that most H5N1 viruses induce high cytokine responses in human macrophages, whereas some H5N1 viruses induce only a low level of cytokine production similar to that induced by seasonal viruses.

Methods. To identify the viral molecular determinants for cytokine induction of H5N1 viruses in human macrophages, we generated a series of reassortant viruses between the high cytokine inducer A/Vietnam/UT3028II/03 clone 2 (VN3028IIcl2) and the low inducer A/Indonesia/UT3006/05 (IDN3006) and evaluated cytokine expression in human macrophages.

Results. Viruses possessing the acidic polymerase (PA) gene of VN3028IIcl2 exhibited high levels of hypercytokinemia-related cytokine expression in human macrophages, compared with IDN3006, but showed no substantial differences in viral growth in these cells. Further, the PA gene of VN3028IIcl2 conferred enhanced virulence in mice.

Conclusions. These results demonstrate that the PA gene of VN3028IIcl2 affects cytokine production in human macrophages and virulence in mice. These findings provide new insights into the cytokine-mediated pathogenesis of H5N1 infection in humans.

Keywords. H5N1 virus; Hypercytokinemia; cytokine; human macrophages; virulence; Microarray; Immune response.

Highly pathogenic avian influenza A virus subtype H5N1 (hereafter, "H5N1") have been circulating among wild birds and domestic poultry worldwide since 2003 [1, 2]. The total number of laboratory-confirmed cases of human H5N1 infection has climbed to >600 cases, with a mortality rate of 60%, posing a true threat to human health [3]. Although the high pathogenicity of these viruses is not completely understood, hypercytokinemia and systemic viral replication have been reported for patients infected with these viruses [4–9].

Alveolar macrophages are considered central players in both innate and adaptive immune responses to respiratory infection and can be infected with H5N1

Received 7 March 2012; accepted 14 June 2012; electronically published 4 October 2012.

Correspondence: Yoshihiro Kawaoka, DVM, PhD, Institute of Medical Science, University of Tokyo, Shirokanedai 4-6-1, Minato-ku, Tokyo 108-8639, Japan (kawaoka@ims.u-tokyo.ac.jp).

The Journal of Infectious Diseases 2013;207:262–71

DOI: 10.1093/infdis/jis523

viruses [10]. In in vitro studies, human monocyte–derived macrophages infected with H5N1 viruses produced higher levels of cytokines than those infected with seasonal viruses, suggesting cytokine production contributes to the high pathogenicity of H5N1 viruses in humans [1, 11–15]. However, we previously found that some H5N1 viruses induce a level of cytokine production similar to that induced by seasonal viruses in human monocyte–derived macrophages [16], indicating that the ability to induce cytokines is virus-strain dependent.

Previous findings regarding the role of nonstructural protein 1 (NS1) in cytokine induction are controversial; in one study, NS1 was shown to affect cytokine production in human macrophages [13], whereas another study was unable to confirm NS1's contribution to cytokine induction in these cells [17]. PB2-E627K, which is widely known as a mutation that enhances viral growth in mammalian cells and some mammals, is reported to enhance cytokine production [13, 18]. Thus, determining the potential molecular markers that enhance cytokine production could extend our knowledge of the basis for the high virulence of H5N1 viruses in humans.

We previously evaluated the ability of several H5N1 viruses to induce cytokines in human macrophages and found that A/Vietnam/UT3028II/03 clone 2 (VN3028IIcl2) was a high cytokine inducer and A/Indonesia/UT3006/05 (IDN3006) a low cytokine inducer [16]. Here, we generated a series of reassortant viruses between these 2 viruses and attempted to identify the viral molecular determinants that confer high cytokine induction in human macrophages. Further, to reveal the molecular networks affected by the virus infection, we examined the entire gene transcriptional profiles in human macrophages by using microarray analysis. To clarify whether differential expression of cytokines mediated by H5N1 viruses contributes to pathogenicity in mammals, we compared the virulence in mice infected with the high cytokine inducer to that in mice infected with the low cytokine inducer.

MATERIALS AND METHODS

Ethics Statement

Our research protocol for the use of human-derived macrophages was approved by the Research Ethics Review Committee of the Institute of Medical Science, the University of Tokyo (approval numbers 18-15-0129 and 19-24-200430). Our research protocol for the use of mice followed the University of Tokyo's Regulations for Animal Care and Use, which was approved by the Animal Experiment Committee of the Institute of Medical Science, the University of Tokyo (approved numbers 19–29).

Cells

A549 and HEK293T cells were maintained in Dulbecco's modified Eagle's medium (DMEM) with 10% fetal calf serum. Madin-Darby canine kidney (MDCK) cells were maintained in minimal essential medium supplemented with 5% newborn calf serum. Human monocyte–derived macrophages were prepared as described previously [16]. Briefly, peripheral blood mononuclear cells were independently separated from the buffy coat of healthy donors. Monocytes were purified by adherence and were allowed to differentiate for 14 days in Roswell Park Memorial Institute (RPMI) 1640 medium supplemented with 5 ng/mL of recombinant human granulocyte-macrophage colony-stimulating factor and 10% human serum derived from the corresponding blood donors. All cells were cultured at 37°C in 5% CO_2.

Viruses

In this study, we used 2 H5N1 viruses with different cytokine induction abilities: A/Vietnam/UT3028II/03 clone 2 (VN3028IIcl2, clade 1) and A/Indonesia/UT3006/05 (IDN3006, clade 2.1.3). Viruses were isolated in MDCK cells, and virus stocks were prepared from the supernatants of MDCK cells.

Plasmid Constructs and Reverse Genetics

Reverse genetics systems for the VN3028IIcl2 and IDN3006 viruses were established as previously described [19]. Briefly, the complementary DNA of genes from these viruses were cloned into the pHH21 vector. The 8 plasmids for the synthesis of viral RNA and 4 expression plasmids for IDN3006 or VN3028IIcl2 virus-derived basic polymerase 2 (PB2), basic polymerase 1 (PB1), acidic polymerase (PA), and nucleoprotein (NP) proteins were transfected into HEK293T cells. Two days later, the supernatant of the transfected cells was harvested and used to infect MDCK cells for the preparation of virus stocks. All virus stocks were sequenced to ensure the absence of unwanted mutations and were titrated by using the plaque assay with MDCK cells prior to use.

Virus Infection of Human Macrophages

Differentiated macrophages were seeded on 24-well plates (BD Falcon), with 1×10^5 cells per well. Cells were infected with viruses at a multiplicity of infection of 2. The virus inoculum was removed, and the cells were washed 3 times and then incubated in serum-free RPMI 1640 medium supplemented with 0.3% bovine serum albumin. At 6, 12, and 24 hours after infection, the supernatant was collected for virus titration and cytokine measurement; the cells were collected for use in viral gene and protein expression assays.

Virus Infection of Human Pulmonary Epithelial Cells

A549 cells were seeded on 6-well plates, with 7.5×10^5 cells per well. Cells were infected with viruses at a multiplicity of infection of 0.0001. The virus inoculum was removed, and the cells were washed 3 times and then incubated in serum-free DMEM supplemented with 0.3% bovine serum albumin. At 6, 12, 24, 48, 72, 96, and 144 hours after infection, viruses in the

supernatants were collected and titrated by means of plaque assays in MDCK cells.

Cytokine Measurements

The concentrations of 7 cytokines (interleukin-6 [IL-6], CXCL10 [IP-10], CCL3 [MIP-1α], CCL4 [MIP-1β], CCL5 [RANTES], tumor necrosis factor α [TNF-α], and CXCL9 [MIG]) in supernatants from human macrophages infected with H5N1 viruses were determined by using the Bio-Plex human x-plex (Bio-Rad Laboratories) and by using the Bio-Plex protein array system (Bio-Rad Laboratories) according to the manufacturer's instructions.

RNA Isolation and Integrity

Infected cells were lysed with TRIzol Reagent (Invitrogen), and chloroform-isoamyl alcohol (5:1) was added. The cells were then vortexed and centrifuged for 15 min at 12 000 × *g* at 4°C. The resulting aqueous layer was subjected to RNA extraction by using RNeasy Mini kit columns (Qiagen) according to the manufacturer's instructions. Isolated total RNA integrity was assessed by determining UV 260/280 absorbance ratios and by examining 28S/18S ribosomal RNA bands with an Agilent 2100 bioanalyzer (Agilent Technologies) according to the manufacturer's instructions. Only samples with high-quality RNA (ie, those with RNA integrity numbers >9.0) were used for microarray analysis.

Microarray Analysis and Bioinformatics

Cy3-labeled complementary RNA probe synthesis was initiated with 50 ng of total RNA by using the Agilent Low Input Quick Amp Labeling kit, one color (Agilent Technologies). The Agilent SurePrint G3 Human GE 8 × 60 K microarrays (G4851) were used according to the manufacturer's instructions. Slides were scanned with an Agilent's High-Resolution Microarray Scanner, and image data were processed by using Agilent Feature Extraction software, version 10.7.3.1. All data were subsequently uploaded into GeneSpring GX, version 11.5, for data analysis. In accordance with proposed MIAME (minimum information about a microarray experiment) standards, microarray data gained in this study are publically available at the Gene Expression Omnibus (GEO) database (http:www.ncbi.nlm.nih.gov/geo/) under the accession number GSE40711. For the microarray data analysis, each gene expression array data set was normalized to the in silico pool for mock-infected cells (n = 3).

Statistically significant differences in gene expression between IDN3006 and VN3028IIcl2 and between IDN3006 and IDN3006/cl2PA were determined by using 1-way analysis of variance (ANOVA) ($P < .05$) with the Tukey honestly significant difference (HSD) post hoc test and the Benjamini-Hochberg false discovery rate correction. Differentially expressed genes were further filtered to include genes whose expression changed at least 2.0-fold relative to the level in the IDN3006-infected group. Only the genes whose expression showed at least 2.0-fold changes and statistical significance ($P < .05$) in 2 pairs of comparisons involving IDN3006 versus VN3028IIcl2 and IDN3006 versus IDN3006/cl2PA were assigned to a Gene Ontology group or were uploaded into Ingenuity Pathway Analysis (IPA; Ingenuity Systems) to identify the functions and pathways that were enriched in the gene set. To identify the gene network that enriched the differentially expressed genes, genes were connected in a de novo network based on known interactions in IPA. Genes that were not directly or indirectly connectable to each other were not analyzed further. For all analysis, *P* values were calculated by using the Fisher exact test to identify biological functions and pathways that were significant ($P < .05$).

Quantitative Real-Time Polymerase Chain Reaction (PCR) Analysis

Quantitative real-time PCR was performed to determine the expression levels of viral PA, hemagglutinin (HA), NP, matrix (M), and NS genes. RNA was reverse-transcribed with oligonucleotide dT and SuperScript III reverse transcriptase (Invitrogen). Quantitative real-time PCR was conducted with the SYBR Green PCR master mix (Invitrogen) and performed on the ABI7900HT Fast Real-Time PCR System platform. Target gene messenger RNA (mRNA) levels were normalized to 18S human ribosomal RNA according to the $2^{-\Delta\Delta Ct}$ calculation [20]. Primer sequences are available on request.

Western Blotting

Infected cells were lysed with 2 × sample buffer (Invitrogen), and samples were loaded onto precast gels for 4%–20% sodium dodecyl sulfate–polyacrylamide gel electrophoresis (Bio-Rad Laboratories). Proteins were transferred electrophoretically to polyvinylidene fluoride membrane (Millipore) in transfer buffer (100 mM Tris, 190 mM glycine, and 10% methanol). The membranes were blocked for 1 hour at room temperature with Blocking One (Nacalai Tesque) and were then incubated with primary antibodies for 1 hour at room temperature. Anti-PA and anti-NS1 mouse monoclonal antibodies (1:10 000) and anti-H5N1 rabbit polyclonal antibodies (1:10 000) for detection of HA, NP, and M1 were used. After being washed 3 times with phosphate-buffered saline containing 0.05% Tween-20 (PBS-T), the membranes were incubated with anti-mouse (1:10 000) or anti-rabbit (1:10 000) secondary antibodies conjugated with horse radish peroxidase (GE Healthcare) for 1 hour at room temperature. After 3 more washes with PBS-T, specific proteins were detected by using the ECL Prime Western Blotting Detection System (GE Healthcare). Photography was conducted with the VersaDoc Imaging System (Bio-Rad laboratories).

Minigenome Assay

Human macrophages or A549 cells were transfected with the expression plasmids for PB2, PB1, PA, and NP (0.25 μg each),

pPolI-NP(0)luc2(0) [21], and ptkRluc (0.025 μg each) by using the jetPEI-Macrophage DNA transfection reagent (Polyplus transfection) or the Lipofectamine LTX and Plus Reagent (Invitrogen), respectively. The cells were then harvested 48 or 24 hours after transfection, respectively. Luciferase activity was assessed by using a dual-luciferase reporter assay system (Promega) according to the manufacturer's instructions. *Photinus* luciferase activity was standardized against *Renilla* luciferase activity.

Animal Experiments

Female BALB/c mice aged 5–6 weeks (Japan SLC) were used in the study. To investigate viral pathogenicity in mice, 4 mice per group were anaesthetized with isoflurane and intranasally infected with 50 μL of serial dilutions of viruses, creating doses ranging from 10^0 to 10^3 plaque-forming units (PFU). Mice were monitored daily for morbidity and mortality for up to 14 days after infection. The percentage changes in body weights were calculated by comparing the weight of each mouse at each time point to its weight on day 0. The 50% mouse lethal dose for each virus was calculated by using the Reed-Muench method [22]. To determine virus growth in mouse organs, 9 mice per group were intranasally infected with 10^2 PFU of IDN3006 or IDN3006/cl2PA. Three mice per group were euthanized on days 2, 4, and 7 after infection, and lungs, nasal turbinates, livers, spleens, kidneys, intestines, and brains were collected. Virus in organs was titrated by using plaque assays in MDCK cells.

Statistical Analysis

Statistically significant differences in cytokine expression, virus growth, luciferase activity, and viral mRNA expression were determined by using 1- or 2-way ANOVA with the post hoc Tukey HSD test. In using 2-way ANOVA, we first confirmed that there were no interaction effects between 2 factors, and then we determined whether there were statistically significant differences in virus growth or viral mRNA levels among the viruses during infection. Statistically significant differences in mouse survival were determined by using the log-rank test. For all statistical tests, values were considered to be significantly different when the P value was $<.05$.

Accession Numbers

The viral nucleotide sequences described in this study are available from GenBank under the following accession numbers: HM114456 for the PA gene of VN3028IIcl2 and JX235398 for IDN3006.

RESULTS

Contribution of the PA Gene to Cytokine Induction in Human Macrophages

To determine the molecular basis for the induction of cytokines in human macrophages, we used 2 H5N1 viruses that differed in their ability to induce cytokines in human macrophages. We first generated wild-type VN3028IIcl2 (high cytokine inducer) and IDN3006 (low cytokine inducer) by using reverse genetics and confirmed the difference in their abilities to induce cytokines by infecting human monocyte–derived macrophages with them and measuring the expression levels of 7 cytokines (IL-6, IP-10, MIP-1α, MIP-1β, RANTES, TNF-α, and MIG; Figure 1). VN3028IIcl2 induced significantly higher expression levels of all of the cytokines tested than did IDN3006 in human macrophages. To identify the gene segments responsible for the difference in cytokine induction between these 2 viruses, we generated 2 reassortant viruses: VN3028IIcl2(3P + NP), which possesses the polymerase complex genes (PB2, PB1, and PA) and the NP gene from VN3028IIcl2 and its remaining genes from IDN3006, and VN3028IIcl2(HA + NA + M + NS), which possesses the HA, neuraminidase (NA), M, and NS genes from VN3028IIcl2 and its remaining genes from IDN3006. VN3028IIcl2(3P + NP) induced statistically significantly higher expression levels of all of cytokines tested than did IDN3006, whereas VN3028IIcl2 (HA + NA + M + NS) did not (Figure 1*A*). These results indicate that the PB2, PB1, PA, and NP genes contribute to the high cytokine induction property of the VN3028IIcl2 virus in human macrophages.

To identify the gene segments responsible for the high cytokine induction among those that encode the proteins in the ribonucleoprotein complex (ie. PB2, PB1, PA, and NP), we generated a series of reassortants possessing a single gene segment derived from VN3028IIcl2 in the IDN3006 backbone (eg, IDN3006/cl2PB2 indicates a virus that possesses the PB2 gene from VN3028IIcl2 and its remaining 7 genes from IDN3006) and evaluated the cytokine expression levels (Figure 1*B*). The reassortants that possessed the single PB2, PB1, or NP gene from VN3028IIcl2 did not induce cytokine levels similar to those produced by the parental VN3028IIcl2. However, the cytokine expression induced by IDN3006/cl2PA was as high as that induced by VN3028IIcl2; the expression levels of RANTES and TNF-α induced by IDN3006/cl2PA were even statistically significantly higher than those induced by VN3028IIcl2. Thus, the PA gene of VN3028IIcl2 was responsible for the high cytokine induction in human macrophages.

Evaluation of the Effect of Viral Replicative Properties on Cytokine Induction

The PA subunit plays a role in virus replication in infected cells [23, 24]. To evaluate whether the high cytokine induction phenotype of VN3028IIcl2 is linked to high viral replication in infected cells, as observed with viruses possessing the PB2-E627K mutation [13], we compared the replication in human macrophages of IDN3006, VN3028IIcl2, and IDN3006/cl2PA (Figure 2) by determining virus titers, polymerase activity, viral protein (PA, HA, NP, M1, and NS1) expression, and viral

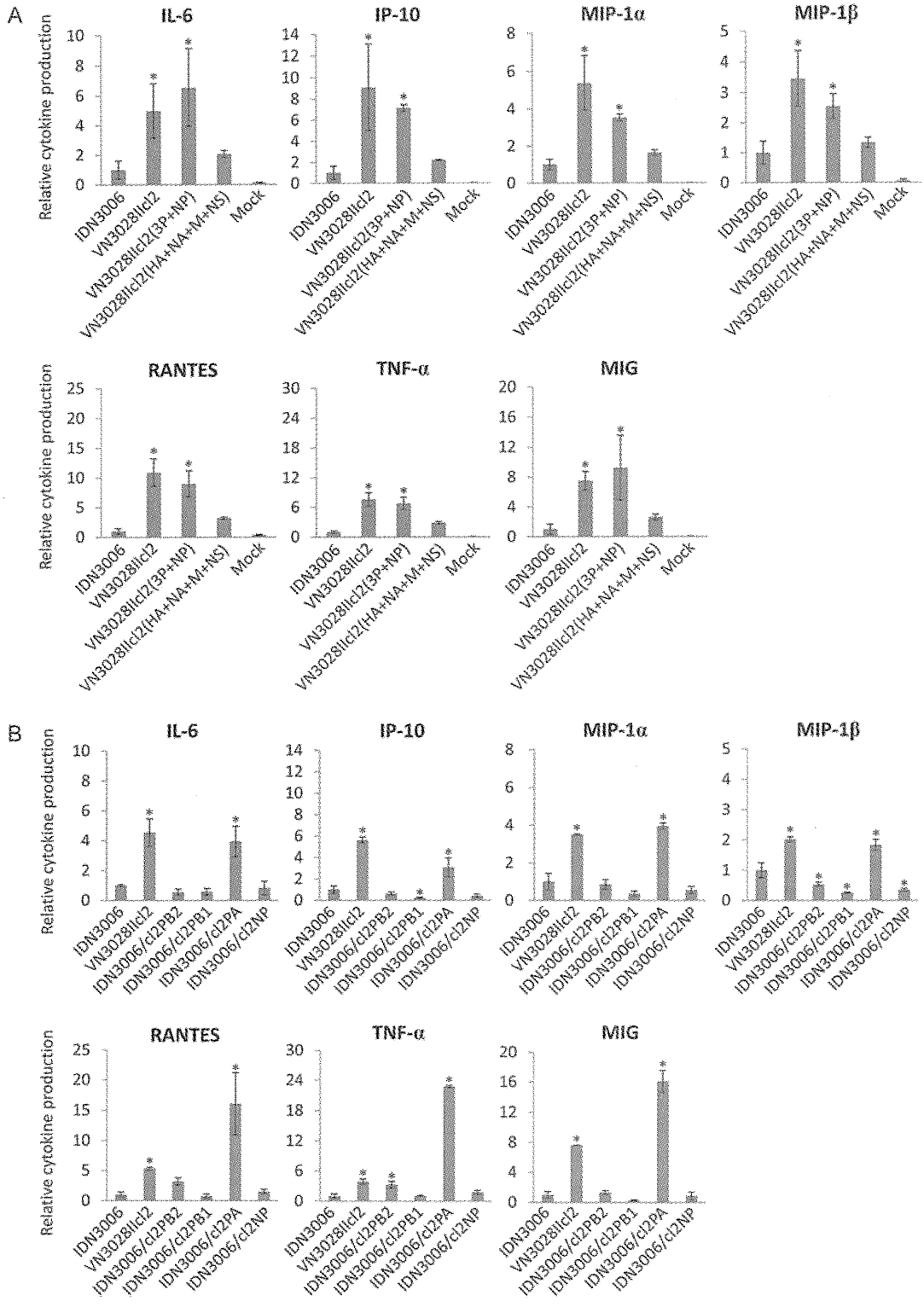

Figure 1. Cytokine production in human macrophages. Human monocyte–derived macrophages were infected with a series of reassortants between IDN3006 and VN3028IIcl2 at a multiplicity of infection of 2. At 12 hours after infection, the supernatants of the infected cells were collected, and the concentrations of 7 cytokines (interleukin-6 [IL-6], CXCL10 [IP-10], CCL3 [MIP-1α], CCL4 [MIP-1β], CCL5 [RANTES], tumor necrosis factor α [TNF-α], and CXCL9 [MIG]) were measured. All values were normalized to the value of IDN3006. *A*, Contributions of a set of 4 viral genes to the cytokine production were evaluated. *B*, Single viral gene segments responsible for the cytokine induction were determined. The values are means ± SD (n = 3). $^*P < .05$, compared with the IDN3006 group (1-way analysis of variance with the post hoc Tukey honestly significant difference test). Abbreviations: HA, hemagglutinin; M, matrix; NA, neuraminidase; NP, nucleoprotein; NS, nonstructural.

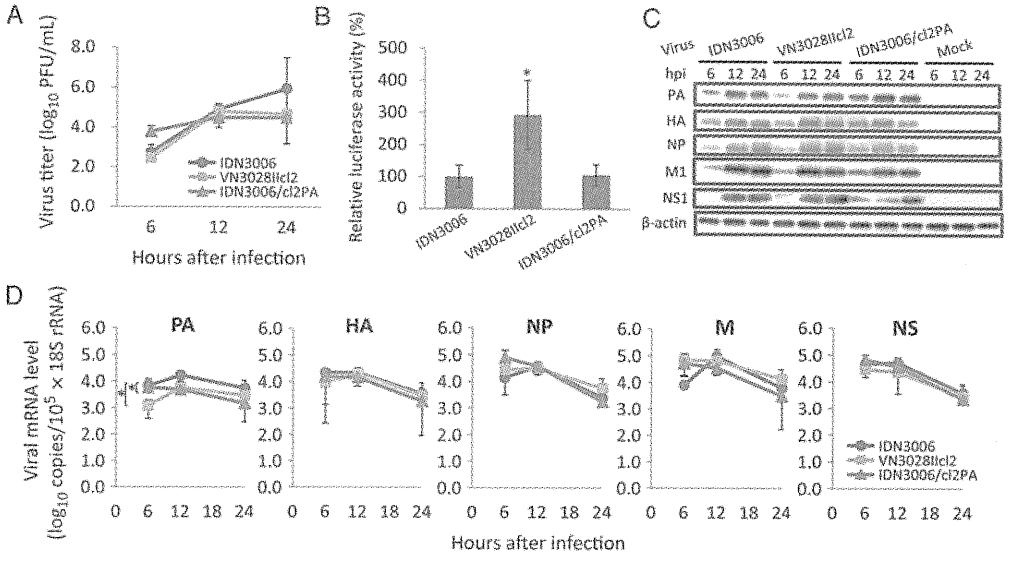

Figure 2. Viral growth properties in human macrophages. Human monocyte–derived macrophages were infected with IDN3006, VN3028IIcl2, or IDN3006/cl2PA at a multiplicity of infection of 2. *A*, At 6, 12, and 24 hours after infection, the virus titers in the supernatants were determined by means of plaque assays in Madin-Darby canine kidney cells. *B*, The 4 viral protein expression plasmids (basic polymerase 2 [PB2], basic polymerase 1 [PB1], acidic polymerase [PA], and nucleoprotein [NP]) of IDN3006, VN3028IIcl2, or IND3006/cl2PA together with pPolINP(0)luc2(0) for the production of virus-like RNA encoding the reporter luciferase gene were transfected into human monocyte–derived macrophages and assayed for luciferase activities 48 hours after transfection at 37°C. The values were standardized to the value for the ribonucleoprotein complex protein activity of IDN3006. *C* and *D*, Viral proteins (PA, hemagglutinin [HA], NP, matrix [M], matrix 1 [M1], nonstructural [NS], and nonstructural 1 [NS1]; *C*) and messenger RNA (mRNA; PA, HA, NP, M, and NS; *D*) expression levels were measured by means of Western blotting and quantitative real-time polymerase chain reaction, respectively. The values are means ± SD (n = 3). **P* < .05 among the 3 groups (2-way analysis of variance with the post hoc Tukey honestly significant difference test).

mRNA gene (PA, HA, NP, M, and NS) expression. Among the 3 viruses tested, there were no statistically significant differences in the virus titers in the supernatants of infected cells, although IDN3006/cl2PA replicated slightly better than IDN3006 or VN3028IIcl2 at 6 hours after infection (Figure 2*A*). Although VN3028IIcl2 showed statistically significantly higher polymerase activity as compared to IDN3006 (Figure 2*B*), IDN3006/cl2PA exhibited polymerase activity similar to that of IDN3006, suggesting that the PA gene of VN3028IIcl2 did not substantially affect the polymerase activity. While only PA gene expression was statistically significantly higher in the IDN3006-infected cells as compared to cells infected with VN3028IIcl2 or IDN3006/cl2PA, there were no substantial differences in the expression levels of other viral proteins or genes tested among the 3 viruses (Figures 2*C* and 2*D*). Thus, we found no appreciable differences in the viral replicative properties of these 3 viruses even though they differed in their cytokine-inducing abilities in human macrophages. These results indicate that the high cytokine induction by VN3028IIcl2 was not related to efficient virus growth in human macrophages.

The Role of the PA Gene of VN3028IIcl2 in the Differential Regulation of Host Genes Involved in Hypercytokinemia

To gain further insights into how the PA gene of VN3028IIcl2 affects cytokine production in human macrophages, we examined all of the gene expression levels in the cells infected with IDN3006, VN3028IIcl2, and IDN3006/cl2PA. The gene expression of IP-10, MIP-1β, RANTES, TNF-α, and MIG confirmed the differential upregulation at the transcriptional level in cells infected with VN3028IIcl2 or IDN3006/cl2PA, compared with those infected with IDN3006 that was observed at the protein level, although the differential upregulation of IL-6 and MIP-1α was confirmed only in cells infected with IDN3006/cl2PA, compared with IDN3006 (Figures 1 and 3*A*). Microarray analyses further identified 129 genes that were statistically significantly differentially expressed in the human macrophages infected with VN3028IIcl2 and IDN3006/cl2PA as compared to IDN3006 (Supplementary Table 1). Gene Ontology analysis revealed that these genes were enriched with cytokine-related genes (Figure 3*B*). IPA network analyses identified a gene network composed of 48 genes that were significantly differentially expressed in the macrophages infected with VN3028IIcl2 and IDN3006/cl2PA as compared to IDN3006 (Figure 3*C*). Of note, this network was enriched with genes related to hypercytokinemia, represented by IFNA4, IFNA8, IFNA14, IFNB1, IL12A, IL29, and CXCL10. These results indicate that the PA amino acid differences are responsible for the differential expression of the various cytokines related to hypercytokinemia at the gene transcriptional level in human macrophages.

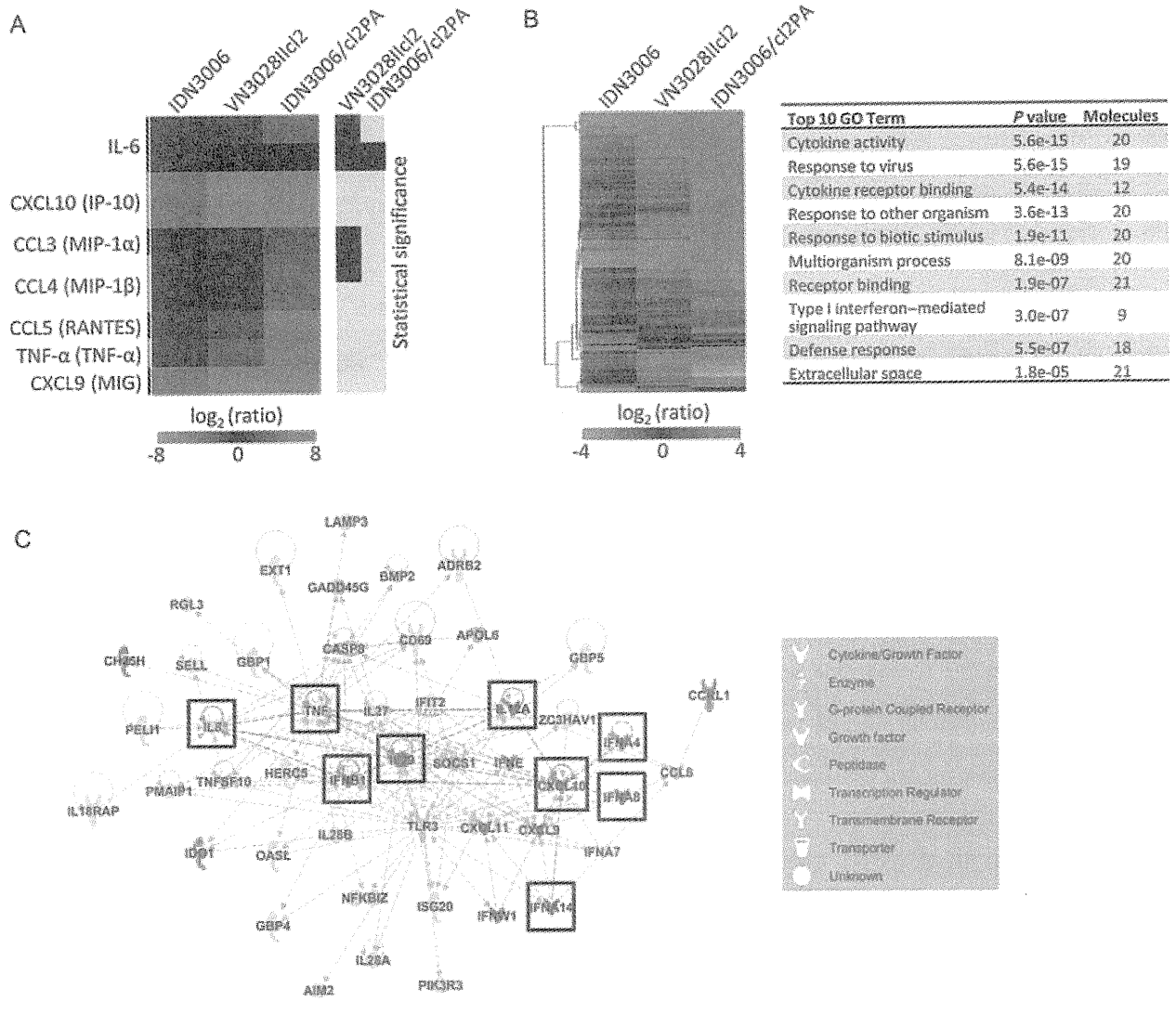

Top 10 GO Term	*P* value	Molecules
Cytokine activity	5.6e-15	20
Response to virus	5.6e-15	19
Cytokine receptor binding	5.4e-14	12
Response to other organism	3.6e-13	20
Response to biotic stimulus	1.9e-11	20
Multiorganism process	8.1e-09	20
Receptor binding	1.9e-07	21
Type I interferon–mediated signaling pathway	3.0e-07	9
Defense response	5.5e-07	18
Extracellular space	1.8e-05	21

Figure 3. Genes differentially expressed between low and high cytokine inducer H5N1 viruses in human macrophages. Human monocyte–derived macrophages were infected with IDN3006, VN3028IIcl2, or IDN3006/cl2PA at a multiplicity of infection of 2. At 6 hours after infection, the cells were harvested and subjected to microarray analysis. *A*, Gene expression levels determined by microarray are shown for the 7 cytokines tested in Figure 1. Yellow indicates $P < .05$, compared with the IDN3006-infected group (1-way analysis of variance [ANOVA] with the Tukey honestly significant difference (HSD) post hoc test). All values were normalized to the values of the mock group. *B*, A total of 129 genes were selected by 1-way ANOVA with the Tukey HSD post hoc test ($P < .05$) and by filtering the genes whose expression changed at least 2.0-fold relative to the level in the IDN3006-infected group. The set of genes differentially regulated in both pairs of VN3028IIcl2 and IDN3006/cl2PA as compared to IDN3006 was functionally annotated by means of Gene Ontology (GO) grouping. Statistical significance was determined by using the Fisher exact test ($P < .05$). *C*, The differentially expressed genes were connected in a de novo network based on known interactions in the Ingenuity Pathway Analysis (IPA) knowledgebase and functionally annotated by use of IPA canonical pathways. Red indicates genes whose expression showed a change of >4.0-fold for both VN3028IIcl2 and IDN3006/cl2PA, relative to IDN3006. Yellow indicates genes whose expression showed a change of >4.0-fold for IDN3006/cl2PA, relative to IDN3006. The genes enriched with the top canonical pathway of "Role of Hypercytokinemia/hyperchemokinemia in the Pathogenesis of Influenza" are boxed.

Contribution of Cytokine Induction to Pathogenicity in Mice

To examine whether the VN3028IIcl2 PA gene that conferred high cytokine induction is associated with pathogenicity in mammals, we compared the pathogenicity in mice of IDN3006 with that of IDN3006/cl2PA. Four mice per group were infected with 10^0–10^3 PFU of each virus, and mortality and morbidity were observed for 14 days after infection (Figure 4). Mice infected with 10^2 PFU of IDN3006/cl2PA exhibited 100% mortality, whereas 75% of mice infected with IDN3006 survived. However, there were no statistically

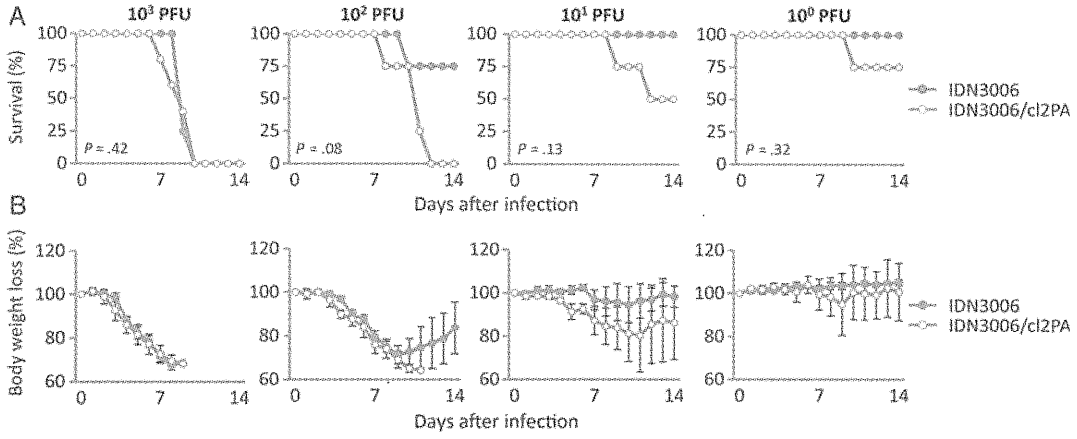

Figure 4. Contribution of the acidic polymerase of VN3028IIcl2 to pathogenicity in mice. Four mice per group were intranasally infected with serially diluted viruses ranging from 10^0 to 10^3 plaque-forming units (PFU) of IDN3006 or IDN3006/cl2PA, and survival (*A*) and body weight changes (*B*) were monitored daily for 14 days after infection. The values are means ± SD (n = 4) for the mice that were alive at each time point. *P* values were determined by using the log-rank test for each pair.

significant differences in mouse survival at any infectious dose tested. The 50% mouse lethal doses of IDN3006 and IDN3006/cl2PA were 2.1×10^2 and 5.9 PFU, respectively. Thus, there was a trend toward increased virulence in mice for IDN3006/cl2PA, compared with IDN3006, indicating that the VN3028IIcl2 PA contributed to virus pathogenicity in mice. These results suggest that the high cytokine induction phenotype contributes to high pathogenicity in mammals.

DISCUSSION

Here, we demonstrated that the PA gene of an H5N1 virus confers high levels of cytokine expression in human monocyte–derived macrophages. We also showed that PA enhances pathogenicity in mammals without altered virus growth properties in human macrophages.

There are 8 amino acid differences in the PA protein between IDN3006 (low cytokine inducer) and VN3028IIcl2 (high cytokine inducer) (Table 1). Yet, we did not find any PA amino acid residues common to either the high or low cytokine inducers examined in our previous study (Table 1) [16]. Although we attempted to identify the amino acid substitutions responsible for the high cytokine production in macrophages, a single amino acid mutation did not substantially change the cytokine induction level (data not shown), suggesting a synergistic effect among the PA amino acids on cytokine induction. The influenza polymerase complex has a role in inhibiting type I interferon in infected cells [25]. Since the PA amino acid differences tested here did not affect the

Table 1. Amino Acid Differences in Acidic Polymerase Between IDN3006 and VN3028IIcl2

Amino Acid	IDN3006	VN3028IIcl2	Low Cytokine Inducers[a]	High Cytokine Inducers[a]	Known Function[b]
90	V	M	V	V/M	...
94	L	I	L/I	I	...
163	I	L	I/L	L	cRNA interaction [26]
327	A	E	A/E	E	...
391	T	R	T/K	K/R	...
520	Y	F	Y/F	F	...
594	G	S	G/S	S	...
653	S	P	S/P	P	PB1 binding [26]

Abbreviations: cRNA, complementary RNA; PB1, basic polymerase 1.

[a] Cytokine induction phenotype was determined in our previous study [16]. Low cytokine inducers include IDN3006 and A/Vietnam/UT31203A/07; high cytokine inducers include VN3028IIcl2 and A/Hong Kong/483/97.

[b] Functions previously reported to be associated with these amino acid positions.

polymerase activity in human macrophages, the host responses in the infected cells may have been affected by the altered anti-interferon activity of the polymerase complex, possibly mediated by PA or by some as yet unknown function of PA.

Virus growth assay revealed that PA was not responsible for the differences between the high and low cytokine inducers with respect to viral transcription, translation, and replication in human macrophages. Interestingly, IDN3006 showed statistically significantly higher growth than IDN3006/cl2PA in human pulmonary epithelial cells (Supplementary Figure 1). Viruses with efficient viral replication in epithelial cells are generally highly pathogenic to mice, represented by viruses with the PB2-E627K mutation, which enhances viral replication in human pulmonary epithelial cells [18]. When we investigated the virus titers in mouse organs, there were no substantial differences between IDN3006 and IDN3006/cl2PA in terms of virus growth in any mouse organ tested (Supplementary Figure 2). Our results, including virus growth, cytokine production, and gene expression in human macrophages, indicate that the ability to induce high levels of cytokines in macrophages, rather than viral replication efficiency in respiratory epithelial cells, may be responsible for enhanced pathogenicity in mice.

In patients infected with H5N1 viruses, high levels of cytokines, represented by MCP-1, MIG, IL-8, IL-10, IL-6, IFN-γ, and RANTES, are generally observed in their sera [6, 9]. Since the PA of a high cytokine inducer was responsible for high levels of these cytokines in macrophages, PA may be a factor in the increased mortality mediated by hypercytokinemia in humans infected with H5N1 viruses. However, both viruses used in this study were isolated from patients who had lethal outcomes, suggesting the involvement of other unknown virulence determinants in the high pathogenicity of H5N1 viruses in humans. Nevertheless, our results have clinical implications for cytokine-mediated pathogenesis in humans infected with H5N1 viruses.

Supplementary Data

Supplementary materials are available at *The Journal of Infectious Diseases* online (http://jid.oxfordjournals.org/). Supplementary materials consist of data provided by the author that are published to benefit the reader. The posted materials are not copyedited. The contents of all supplementary data are the sole responsibility of the authors. Questions or messages regarding errors should be addressed to the author.

Notes

Acknowledgments. We thank Susan Watson for editing the manuscript.

Financial support. This work was supported by a grant-in-aid for Specially Promoted Research and by the Japan Initiative for Global Research Network on Infectious Diseases from the Ministry of Education, Culture, Sports, Science, and Technology, Japan; by a grant-in-aid of Scientific Research from the Ministry of Health, Labor, and Welfare, Japan; by a grant-in-aid for Exploratory Research for Advanced Technology (ERATO) from Japan Science and Technology Agency (JST), Japan; and by National Institute of Allergy and Infectious Diseases Public Health Service Research grants. S. S. and R. T. were supported by Research Fellowships from the Japan Society for the Promotion of Science for Young Scientists.

Potential conflicts of interest. All authors: No reported conflicts.

All authors have submitted the ICMJE Form for Disclosure of Potential Conflicts of Interest. Conflicts that the editors consider relevant to the content of the manuscript have been disclosed.

References

1. Guan Y, Poon LL, Cheung CY, et al. H5N1 influenza: a protean pandemic threat. Proc Natl Acad Sci U S A **2004**; 101:8156–61.
2. Li KS, Guan Y, Wang J, et al. Genesis of a highly pathogenic and potentially pandemic H5N1 influenza virus in eastern Asia. Nature **2004**; 430:209–13.
3. World Health Organization (WHO). Cumulative number of confirmed human cases of avian influenza A(H5N1) reported to WHO. Geneva: WHO, **2012**. http://www.who.int/influenza/human_animal_interface/H5N1_cumulative_table_archives/en/index.html. Accessed 10 September 2012.
4. Hui DS. Review of clinical symptoms and spectrum in humans with influenza A/H5N1 infection. Respirology **2008**; 13(Suppl 1):S10–3.
5. de Jong MD, Bach VC, Phan TQ, et al. Fatal avian influenza A (H5N1) in a child presenting with diarrhea followed by coma. N Engl J Med **2005**; 352:686–91.
6. de Jong MD, Simmons CP, Thanh TT, et al. Fatal outcome of human influenza A (H5N1) is associated with high viral load and hypercytokinemia. Nat Med **2006**; 12:1203–7.
7. Abdel-Ghafar AN, Chotpitayasunondh T, Gao Z, et al. Update on avian influenza A (H5N1) virus infection in humans. N Engl J Med **2008**; 358:261–73.
8. Yuen KY, Chan PK, Peiris M, et al. Clinical features and rapid viral diagnosis of human disease associated with avian influenza A H5N1 virus. Lancet **1998**; 351:467–71.
9. Peiris JS, Yu WC, Leung CW, et al. Re-emergence of fatal human influenza A subtype H5N1 disease. Lancet **2004**; 363:617–9.
10. van Riel D, Munster VJ, de Wit E, et al. H5N1 virus attachment to lower respiratory tract. Science **2006**; 312:399.
11. Cheung CY, Poon LL, Lau AS, et al. Induction of proinflammatory cytokines in human macrophages by influenza A (H5N1) viruses: a mechanism for the unusual severity of human disease?. Lancet **2002**; 360: 1831–7.
12. Lee SM, Gardy JL, Cheung CY, et al. Systems-level comparison of host-responses elicited by avian H5N1 and seasonal H1N1 influenza viruses in primary human macrophages. PLoS One **2009**; 4:e8072.
13. Mok KP, Wong CH, Cheung CY, et al. Viral genetic determinants of H5N1 influenza viruses that contribute to cytokine dysregulation. J Infect Dis **2009**; 200:1104–12.
14. Woo PC, Tung ET, Chan KH, Lau CC, Lau SK, Yuen KY. Cytokine profiles induced by the novel swine-origin influenza A/H1N1 virus: implications for treatment strategies. J Infect Dis **2010**; 201: 346–53.
15. Hui KP, Lee SM, Cheung CY, et al. H5N1 influenza virus-induced mediators upregulate RIG-I in uninfected cells by paracrine effects contributing to amplified cytokine cascades. J Infect Dis **2011**; 204: 1866–78.
16. Sakabe S, Iwatsuki-Horimoto K, Takano R, et al. Cytokine production by primary human macrophages infected with highly pathogenic H5N1 or pandemic H1N1 2009 influenza viruses. J Gen Virol **2011**; 92:1428–34.
17. Monteerarat Y, Sakabe S, Ngamurulert S, et al. Induction of TNF-alpha in human macrophages by avian and human influenza viruses. Arch Virol **2010**; 155:1273–9.
18. Hatta M, Gao P, Halfmann P, Kawaoka Y. Molecular basis for high virulence of Hong Kong H5N1 influenza A viruses. Science **2001**; 293:1840–2.

19. Neumann G, Watanabe T, Ito H, et al. Generation of influenza A viruses entirely from cloned cDNAs. Proc Natl Acad Sci U S A **1999**; 96:9345–50.
20. Livak KJ, Schmittgen TD. Analysis of relative gene expression data using real-time quantitative PCR and the 2(-Delta Delta C(T)) Method. Methods **2001**; 25:402–8.
21. Octaviani CP, Goto H, Kawaoka Y. Reassortment between seasonal H1N1 and pandemic (H1N1) 2009 influenza viruses is restricted by limited compatibility among polymerase subunits. J Virol **2011**; 85:8449–52.
22. Reed LJ, Muench H. A simple method of estimating fifty percent end points. Am J Hyg **1938**; 27:493–7.
23. Honda A, Ishihama A. The molecular anatomy of influenza virus RNA polymerase. Biol Chem **1997**; 378:483–8.
24. Huang TS, Palese P, Krystal M. Determination of influenza virus proteins required for genome replication. J Virol **1990**; 64: 5669–73.
25. Iwai A, Shiozaki T, Kawai T, et al. Influenza A virus polymerase inhibits type I interferon induction by binding to interferon beta promoter stimulator 1. J Biol Chem **2010**; 285:32064–74.
26. Naffakh N, Tomoiu A, Rameix-Welti MA, van der Werf S. Host restriction of avian influenza viruses at the level of the ribonucleoproteins. Annu Rev Microbiol **2008**; 62:403–24.

MAJOR ARTICLE

Molecular Mechanisms Underlying Oseltamivir Resistance Mediated by an I117V Substitution in the Neuraminidase of Subtype H5N1 Avian Influenza A Viruses

Ryo Takano,[1,a] Maki Kiso,[1,a] Manabu Igarashi,[5,a] Quynh Mai Le,[7] Masakazu Sekijima,[3] Kimihito Ito,[5] Ayato Takada,[6] and Yoshihiro Kawaoka[1,2,4,8]

[1]Division of Virology, Department of Microbiology and Immunology, and [2]International Research Center for Infectious Diseases, Institute of Medical Science, University of Tokyo, [3]Global Scientific Information and Computing Center, Tokyo Institute of Technology, Tokyo, [4]ERATO Infection-Induced Host Response Project, Japan Science and Technology Agency, Saitama and [5]Division of Bioinformatics; and [6]Division of Global Epidemiology, Hokkaido University Research Center for Zoonosis Control, Sapporo, Japan; [7]National Institute of Hygiene and Epidemiology, Hanoi, Vietnam; and [8]Department of Pathobiological Sciences, School of Veterinary Medicine, University of Wisconsin–Madison

Background. The neuraminidase (NA) inhibitor oseltamivir is widely used to treat patients infected with influenza viruses. An Ile-to-Val change at position 117 in influenza A virus subtype H5N1 NA (NA-I117V) confers a reduction in susceptibility to oseltamivir carboxylate. However, the in vivo relevance and molecular basis of the decreased sensitivity mediated by this mutation are poorly understood.

Methods. We created single-point-mutant viruses with 3 genetically different backgrounds (ie, 1 belonging to clade 1 and 2 belonging to clade 2.3.4) and evaluated the effects of the I117V mutation on oseltamivir susceptibility in vitro, in vivo, and in silico.

Results. The NA-I117V mutation conferred a slight reduction in susceptibility to oseltamivir in vitro (1.3- to 6.3-fold changes), although it did not substantially compromise NA enzymatic activity. Mice infected with I117V virus exhibited reduced susceptibility to oseltamivir and decreased survival in 2 of 3 virus pairs tested. Molecular dynamics simulations revealed that I117V caused the loss of hydrogen bonds between an arginine at position 118 and the carboxyl group of oseltamivir, leading to a lower binding affinity for oseltamivir.

Conclusions. Our findings provide new insight into the mechanism of NA-I117V–mediated oseltamivir resistance in highly pathogenic H5N1 avian influenza viruses.

Keywords. Influenza A virus; H5N1; Oseltamivir; Neuraminidase; I117V mutation; Molecular dynamics simulation.

Since 2003, highly pathogenic subtype H5N1 avian influenza A viruses have circulated among poultry and wild birds in Asia, Africa, and Europe [1]. As of 10 August 2012, in addition to frequent avian outbreaks, >600 cases of H5N1 infections in humans have been reported [2]. Since these viruses are currently unable to transmit efficiently among humans, human infections have been limited to close contact with infected poultry, with a few exceptions [3]. Yet, unlike seasonal subtype H1N1 influenza A virus, seasonal subtype H3N2 influenza A virus, or 2009 pandemic subtype H1N1 influenza A virus, the illness associated with H5N1 viruses in humans follows an unusually aggressive clinical course, with rapid deterioration and high mortality (approximately 60%) [2].

The neuraminidase (NA) inhibitor oseltamivir is commonly used in clinical practice to treat influenza virus infections in patients. NA inhibitors interrupt the virus replication cycle by preventing the release of viruses from infected cells. They were designed to target the sialic acid–binding pocket of NA, which is composed of 19 conserved residues (8 functional

Received 15 May 2012; accepted 23 July 2012; electronically published 10 October 2012.

[a]R. T., M. K., and M. I. contributed equally to this work.

Correspondence: Yoshihiro Kawaoka, Department of Microbiology and Immunology, Institute of Medical Science, University of Tokyo, 4-6-1 Shirokanedai, Minato-ku, Tokyo 108-8639, Japan (kawaoka@ims.u-tokyo.ac.jp).

The Journal of Infectious Diseases 2013;207:89–97

DOI: 10.1093/infdis/jis633

residues [R118, D151, R152, R224, E276, R292, R371, and Y406; N2 numbering] and 11 framework residues [E119, R156, W178, S179, D198, I222, E227, H274, E277, N294, and E425; N2 numbering]) [4, 5]. Therefore, mutations at these positions can confer drug resistance [6, 7].

A previous report raised the possibility that genetic variation, represented by E248G and Y252H, in the absence of any drug-selective pressure can lead to significant changes in NA inhibitor sensitivity [8]. McKimm-Breschkin et al [9] reported that some H5N1 viruses isolated in Cambodia and Indonesia are less sensitive than 2004 clade 1 viruses to oseltamivir, yet none of the NA amino acid changes detected in these viruses was known to confer oseltamivir resistance. These findings suggest that the decrease in sensitivity may be due to drift mutations rather than to selective pressure posed by oseltamivir per se. Thus, viruses could acquire reduced anti-NA drug sensitivity by not only drug-selective pressure but also natural genetic variation [10]. In either case, with increasing clinical use and stockpiling of NA inhibitors for pandemic preparedness, it is important to define all mutations that could confer resistance to NA inhibitors.

Recently, a novel substitution, isoleucine to valine at position 117 (I117V) in the NA protein (NA-I117V) of an avian isolate was reported to slightly increase the half maximal inhibitory concentration (IC_{50}) of oseltamivir carboxylate in vitro (from 5.1-fold to approximately 16-fold) [11, 12]. However, the clinical relevance of this approximate 10-fold decrease in sensitivity is unknown. Although variations at this position (I117V/M) have been reported to reduce susceptibility to oseltamivir in 2009 pandemic H1N1 viruses [13, 14], the molecular mechanisms underlying the reduced sensitivity to oseltamivir caused by NA-I117V remain poorly understood. Here, to elucidate the effects of the NA-I117V substitution on susceptibility to oseltamivir, we generated recombinant viruses with this substitution in 3 genetically different virus backgrounds and compared their NA enzymatic activity and susceptibility to oseltamivir in vitro and in vivo. To reveal the mechanisms underlying any conformational changes in the NA enzymatic site induced by the I117V mutation, we also performed molecular dynamics analysis to assess the binding stability of NA to oseltamivir carboxylate.

MATERIALS AND METHODS

Details of the cells, viruses, plasmid-based reverse genetics, statistical analysis, and other experimental procedures can be found in the Supplementary materials.

NA Inhibition Assay

The sensitivity of viral NA to oseltamivir carboxylate was evaluated by using an NA enzyme inhibition assay based on the method of MUNANA. Virus dilutions containing between 800 and 1200 fluorescence units were used in this assay. Diluted virus and the drug (0.01 nM–1 mM in 33 mM 2-[N-morpholino] ethanesulfonic acid [pH 6.0] containing 4 mM $CaCl_2$) were mixed and incubated for 30 minutes at 37°C, followed by addition of the substrate. After 1 hours at 37°C, the reaction was stopped, and fluorescence was quantified. The relationship between the concentration of inhibitor and the percentage of fluorescence inhibition was determined, and IC_{50} values for NA activity were obtained by extrapolating those findings.

Therapeutic Efficacy of Oseltamivir in Mice

Female BALB/c mice aged 5–6 weeks (Japan SLC, Shizuoka, Japan) were used in the experiment. Prior to evaluating the efficacy of oseltamivir in mice, we anesthetized 4 mice per group by using sevoflurane inhalation and intranasally inoculated them with serial 10-fold diluted virus in 50 mL of phosphate-buffered saline to calculate the 50% mouse lethal dose (MLD_{50}). To study the efficacy of oseltamivir, 16 mice per group were infected with 10 MLD_{50} of viruses and then orally mock treated or treated with 30, 100, or 300 mg/kg oseltamivir phosphate 2 hours after infection and then twice daily for 5 days. Mice were monitored daily for morbidity and mortality for 21 days after infection. On days 3 and 6 after infection, 3 mice per group were euthanized, and brain, nasal turbinate, lung, spleen, liver, kidney, and jejunum were collected. These tissue samples were subsequently homogenized in Eagle's minimal essential medium containing 0.3% bovine serum albumin at a final concentration of 10%, and cellular debris was removed by centrifugation at 5000 *g* for 5 minutes. Virus in the supernatant was then determined by using plaque assays involving Madin-Darby canine kidney cells.

Molecular Dynamics Simulations

The initial coordinates of wild-type VN1203 NA with oseltamivir were taken from the cocrystal structure (PDB code 2HU4). The structure of the NA-I117V mutant with oseltamivir was generated by replacing isoleucine 117 in the wild-type complex with valine by using the LEAP module in the AMBER 11 software suite [15]. Protonation states of the ionizable residues were assigned at pH 6.5 by using the PDB2PQR web server [16]. All missing hydrogen atoms were added by using LEAP. The geometry and electrostatic potential of oseltamivir were calculated at the HF/6-31G(d) level with Gaussian 03 [17]. On the basis of the results of these calculations, partial charges of oseltamivir were determined with the restrained electrostatic potential procedure [18], using the Antechamber program of AMBER 11 [19]. The FF99SB force field and the generalized AMBER force field were applied for each NA and for oseltamivir, respectively [20, 21]. The total charges of the NA-oseltamivir complexes were neutralized by the addition of sodium counterions. Then, the systems were solvated in a truncated octahedral box of TIP3P water molecules with a

distance of at least 10 Å around the complex. The total atoms were 30 400 for both the wild-type and mutant NA systems. All energy minimization and molecular dynamics (MD) simulations were performed by using the PMEMD module in AMBER 11, with a cutoff radius of 12 Å for the nonbonded interactions. The locations of hydrogen atoms, water molecules, and counterions were optimized to remove bad contacts. Then, each system was energy minimized without any constraints by using the steepest descent method for 500 steps, followed by the conjugate gradient method for 1500 steps. After minimization, the system was gradually heated from 0 K to 300 K at 5 ps per 50 K with a force constant of 1.0 kcal/mol·Å^2. An additional 2 rounds of MD (50 ps each at 300 K) were performed with decreasing restraint weight reduced from 0.5 to 0.1 kcal/mol·Å^2. Then, 2.5 ns of unrestrained MD at 300 K was run to equilibrate the system. Finally, a 2.5-ns production run was performed, and the production trajectories were collected every 1 ps. All MD simulations were performed using the NPT ensemble and the Berendsen algorithm [22] to control temperature and pressure. The time step was 2 fs, and the SHAKE algorithm [23] was used to constrain all bond lengths involving hydrogen atoms. Long-range electrostatic interactions were treated using the particle mesh Ewald method [24]. Binding free energies were calculated using the script of the molecular mechanics/Poisson-Boltzmann surface area (MM/PBSA) method in AMBER 11 (MM/PBSA.py), which uses a single-trajectory approach. Snapshots were taken every 5 ps for the enthalpy estimates and every 350 ps for the entropy estimates on the free calculations. Calculation of the binding free energy between an NA mutant and oseltamivir by using the MM/PBSA method was described in detail previously [25–28].

RESULTS

NA Enzymatic Activity of H5N1 Viruses Possessing a Single Point Mutation at Position 117

To investigate the prevalence of H5N1 virus strains that possess the NA-I117V mutation, we reviewed the H5N1 NA sequences in the public database. Of the 2691 virus strains reviewed, variation at this position was found in at least 58 strains (approximately 2%), the HAs of which differed such that they covered a broad range of clades, including 0, 1, 2.1.1, 2.2, 2.3.2, 2.3.4, and 9 (Supplementary Table 1). In our surveillance study in Vietnam from 2007–2008, we found the NA-I117V substitution in 2 poultry isolates: A/duck/Vietnam/TY103/2007 (Bacgiang province isolate) and A/duck/Vietnam/TY114/2007 (Thaibinh province isolate). This substitution was also found in a clinical specimen from a patient infected with an H5N1 virus in Hai Duong province, Vietnam, in 2008 (A/Vietnam/UT31412II/2008) [29]. We then studied the contribution of NA-117 to oseltamivir resistance by using the following 3 genetically different viruses: A/Vietnam/1203/2004 (VN1203, clade 1), A/duck/Vietnam/TY114/2007 (TY114, clade 2.3.4), and A/Vietnam/UT31412II/2008 (VN31412, clade 2.3.4), none of which have any known oseltamivir resistance–conferring mutations. Of these 3 viruses, VN1203 possessed NA-117I, whereas TY114 and VN31412 had NA-117V, as stated above. We therefore generated 3 virus pairs, each differing by only the amino acid at position NA-117: VN1203 (wtNA-117I) and VN1203 (NA-117V), TY114 (wtNA-117V) and TY114 (NA-117I), and VN31412 (wtNA-117V) and VN31412 (NA-117I).

We then evaluated the effect of the NA-I117V substitution on NA enzymatic activity by using MUNANA substrate (Figure 1*A–C*). We found that viruses possessing valine at position 117 in NA exhibited statistically significantly higher enzymatic activity than did those possessing isoleucine at this position, regardless of the virus backbone. Next, we tested the biologic effect of the NA-I117V substitution in the hemagglutination-elution assay with chicken erythrocytes [30] and found that the NA-I117V substitution did not influence the ability of NA to elute virus from erythrocytes in any of the 3 virus backbones tested (Figure 1*D*). Thus, the NA-I117V mutation did not compromise the NA enzymatic activity; rather, it increased it regardless of the virus backbone tested.

Effects of NA-I117V on Oseltamivir Carboxylate Susceptibility In Vitro

To evaluate the effect of the NA-I117V substitution on susceptibility to oseltamivir in vitro, the IC_{50} values of oseltamivir carboxylate were measured by using a fluorometric NA inhibition assay (Figure 1*E–G*; Table 1). Clade 2.3.4 viruses (TY114 and VN31412 pairs) exhibited higher IC_{50} values than did the clade 1 virus (VN1203 pair), as previously reported [9]. The VN1203 NA-117V and wild-type VN31412 (wtNA-117V) viruses exhibited 6.3- and 3.4-fold higher IC_{50} values, respectively, than those of viruses possessing isoleucine, whereas wild-type TY114 (wtNA-117V) showed a mere 1.3-fold higher IC_{50} value than its 117I mutant. These results indicate that the I117V substitution confers slightly reduced susceptibility to oseltamivir carboxylate in vitro, the degree of which was dependent on the virus backbone.

Effects of NA-I117V on the Therapeutic Efficiency of Oseltamivir Phosphate in a Mouse Model

We next assessed the effect of the NA-I117V substitution on the therapeutic efficacy of oseltamivir in mice. Prior to treatment, we calculated the MLD_{50} values to compare the pathogenicity of the virus pairs in mice (Table 1). Although the VN31412 pair was more virulent in mice than were the other 2 virus pairs, there were no substantial differences in MLD_{50} values within virus pairs, suggesting a limited contribution of the I117V substitution to pathogenicity in mice.

To evaluate the effect of the NA-I117V substitution on oseltamivir susceptibility in mice, mice were infected with 10

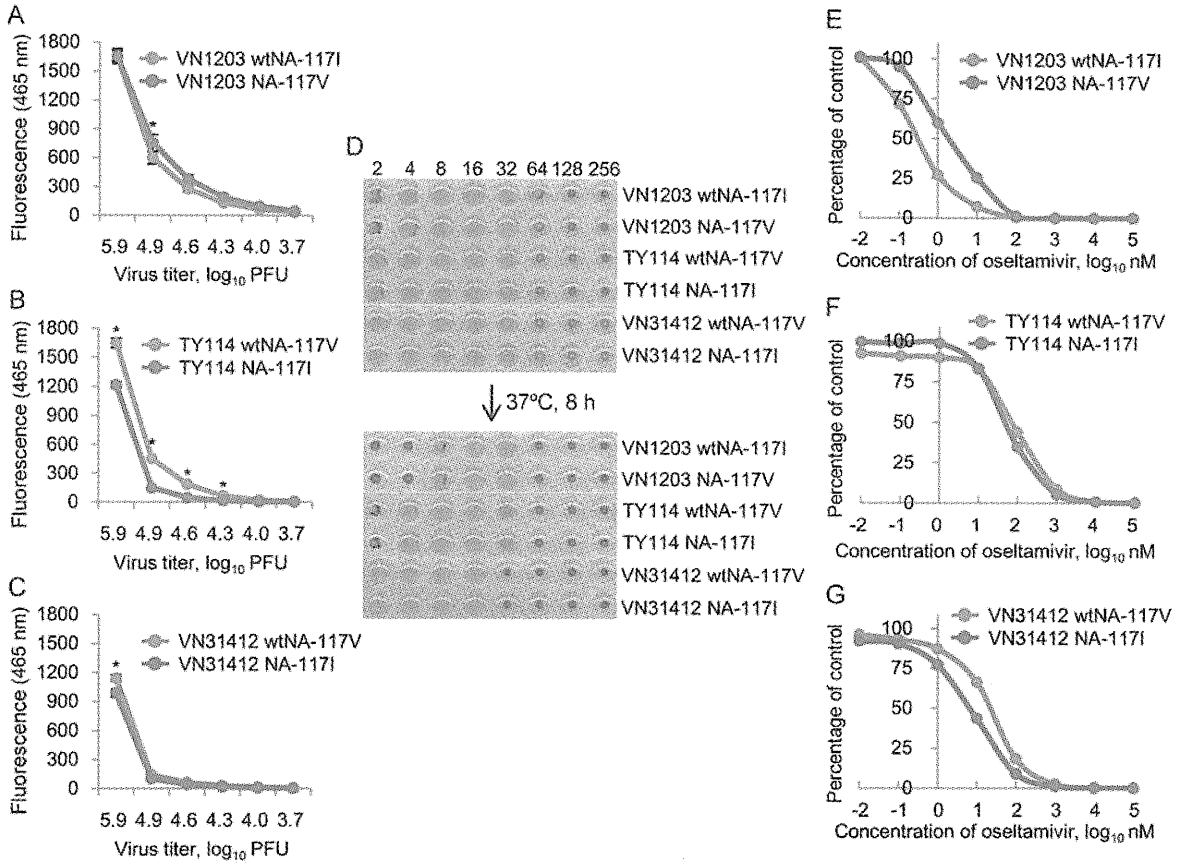

Figure 1. Neuraminidase (NA) activity of subtype H5N1 influenza A viruses and the inhibitory effect of oseltamivir carboxylate. Three H5N1 virus pairs were evaluated for NA enzymatic activity, hemagglutination-elution activity, and NA sensitivity to oseltamivir carboxylate. *A–C,* NA enzymatic activity was measured by the method of MUNANA substrates; the values shown represent the means of triplicate experiments. $^*P < .05$, significant difference compared with the I117I viruses. *D,* Serial 2-fold dilutions of the viruses were incubated with equal volumes of 0.5% chicken erythrocytes at 4°C for 1 hours (top panel), followed by incubation at 37°C for 8 hours (bottom panel). *E–G,* The sensitivity of NA to oseltamivir carboxylate was determined by using MUNANA as a substrate; the values shown represent the means of duplicate experiments.

MLD_{50} of the VN1203 pair and then mock treated or treated with oseltamivir phosphate at a dosage of 30, 100, or 300 mg/kg twice daily for 5 days after infection (Figure 2*A* and 2*B*). In the mice infected with the wild-type VN1203 (wtNA-117I) virus (Figure 2*A*), oseltamivir treatment produced a dose-dependent protective effect against virus dissemination into multiple organs at days 3 and 6 after infection (Table 2). Virus titers in lungs were significantly reduced by the administration of 300 mg/kg oseltamivir at days 3 and 6 after infection (Figure 2*G*). Of the mice infected with the VN1203 NA-117V mutant virus (Figure 2*B*), however, 60% died even when treated with the highest oseltamivir dose, even though oseltamivir reduced viral growth and dissemination (Table 2 and Figure 2*G*). Because a difference in oseltamivir efficacy was observed at the high dose of oseltamivir in mice infected with the VN1203 pair, we also investigated mouse survival for the TY114 and VN31412 pairs at the high dose of oseltamivir. The reduced efficacy of oseltamivir was also observed for the TY114 pair (Figure 2*C,* 2*D,* and 2*H* and Table 2). In mice infected with the VN31412 pair, the therapeutic efficacy was the lowest of all of the viruses tested, and there was no difference in the effect of the I117V substitution on the survival of the mice (Figure 2*E* and 2*F*). These results indicate that, depending on the genetic background of the virus, the NA-I117V substitution confers reduced susceptibility to oseltamivir in mice.

Effects of the NA-I117V on the Interaction Between R118 and Oseltamivir

The cocrystal structure of wild-type VN1203 NA with oseltamivir carboxylate (PDB code 2HU4) shows that the isoleucine at position 117 does not directly interact with oseltamivir (Figure 3*A*). To elucidate the molecular basis of how the I117V substitution causes reduced susceptibility to

Table 1. Fifty Percent Mouse Lethal Dose (MLD_{50}) and Half Maximal Inhibitory Concentration (IC_{50}) Values for Oseltamivir Carboxylate to Wild-Type and Neuraminidase (NA)–Mutant Subtype H5N1 Influenza A Viruses

Virus	Clade	Recombinant Virus	Amino Acid 117 in NA	MLD_{50} (PFU)	IC_{50} (nM)[a]	Ratio of IC_{50} (117V/117I)
A/Vietnam/1203/2004	1	VN1203 wtNA-117I	I	21	0.32	...
		VN1203 NA-117V	V	32	2.0	6.3
A/duck/Vietnam/TY114/2007	2.3.4	TY114 wtNA-117V	V	30	68	1.3
		TY114 NA-117I	I	30	52	...
A/Vietnam/UT31412II/2008	2.3.4	VN31412 wtNA-117V	V	0.59	22	3.4
		VN31412 NA-117I	I	2.1	6.5	...

Abbreviation: PFU, plaque-forming units.

[a] Calculated from the duplicate experiments described in Figure 1*E–G*.

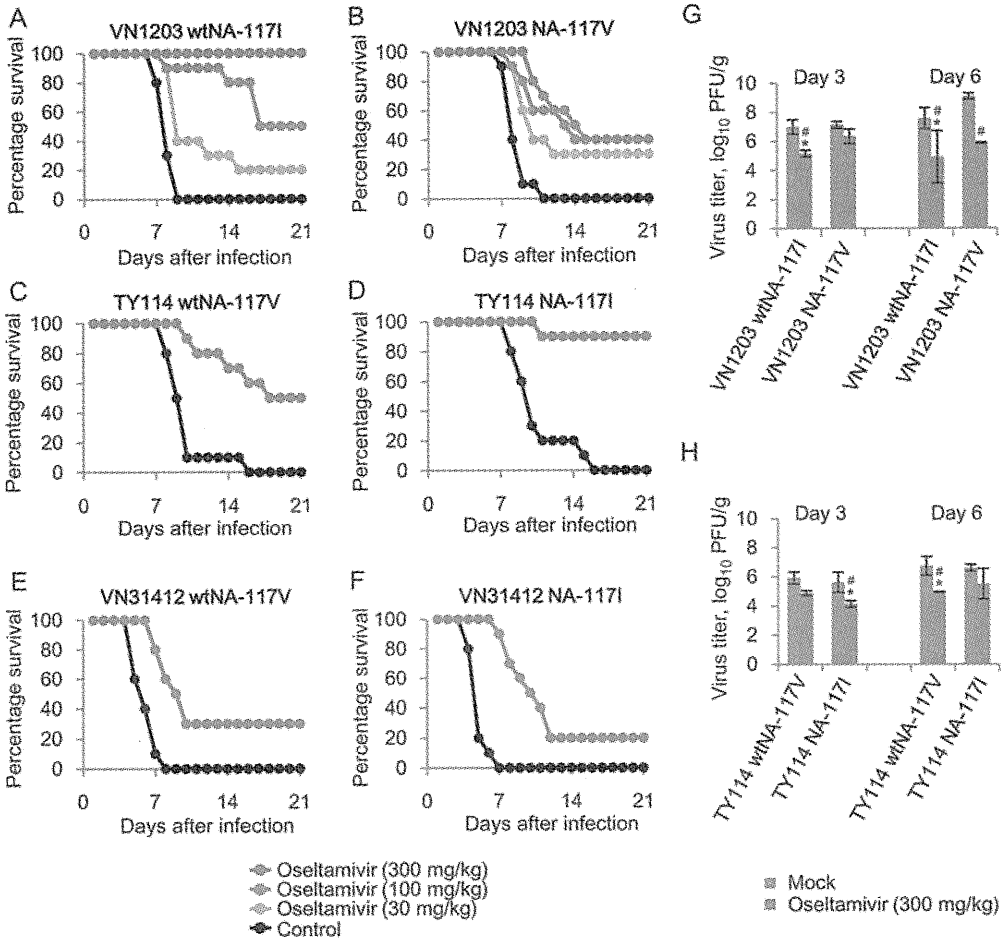

Figure 2. Therapeutic efficacy of oseltamivir phosphate against subtype H5N1 influenza A viruses in mice. Sixteen mice per group were intranasally infected with ten 50% mouse lethal doses of viruses and then given 30, 100, and 300 mg/kg oseltamivir phosphate orally 2 hours after infection and twice daily thereafter for 5 days. Three mice per group were euthanized on days 3 and 6 after infection, and their lungs were collected for virus growth assays. *A–F*, Survival was monitored daily for 21 days, and survival curves were obtained from 10 mice per group. *G* and *H*, Virus titers in lungs are shown; the values are mean ± SD (n = 3). $^{*}P < .05$, significant difference between levels in the lungs of mice infected with virus possessing 117I and those infected with virus possessing 117V.; $^{\#}P < .05$, significant difference between levels in the lungs of mice, mock-treated and treated with oseltamivir phosphate. (1-way analysis of variance with the Tukey multiple comparisons posttest).